Identification Method of Error Motions and Geometric Errors of a Rotary Axis by R-Test

Kenno, Takaaki
Sato, Ryuta
Shirase, Keiichi
Natsume, Shigemasa
Spaan, Henny

(Citation)
International Journal of Automation Technology,14(3):399-408

(Issue Date)
2020-05-05

(Resource Type)
journal article

(Version)
Version of Record

(URL)
https://hdl.handle.net/20.500.14094/90009293

https://doi.org/10.20965/ijat.2020.p0399

Paper:

Identification Method of Error Motions and Geometric Errors of a Rotary Axis by R-Test

Takaaki Kenno*, Ryuta Sato*,†, Keiichi Shirase*, Shigemasa Natsume, and Henny Spaan*****

*Department of Mechanical Engineering, Kobe University
1-1 Rokko-dai, Nada-ku, Kobe 657-8501, Japan
†Corresponding author, E-mail: sato@mech.kobe-u.ac.jp
**P&C Ltd., Yokohama, Japan
***IBS Precision Engineering BV, Eindhoven, Netherlands
[Received September 29, 2019; accepted December 10, 2019]

While evaluating the accuracy of high-precision machine tools, it is critical to reduce the error factors contributing to the measured results as much as possible. This study aims to evaluate both the error motions and geometric errors of the rotary axis without considering the influence of motion error of the linear axis. In this study, only the rotary axis is moved considering two different settings of a reference sphere, and the linear axes are not moved. The motion accuracy of the rotary axis is measured using the R-test device, both the error motions and geometric errors of the rotary axis are identified from the measurement results. Moreover, the identified geometric errors are verified for correctness via measurement with an intentional angular error. The results clarify that the proposed method can identify the error motions and geometric errors of a rotary axis correctly. The method proposed in this study can thus be effective for evaluating the motion accuracy of the rotary axis and can contribute to further improvement of the accuracy of the rotary table.

Keywords: five-axis machine tools, rotary axis, error motion, geometric error, R-test

1. Introduction

Five-axis controlled machine tools with three linear-axes and two rotary-axes can control both the relative position and relative angle between the tool and the workpiece. However, these machine tools exhibit inferior machining accuracy when compared to three-axis controlled machine tools because of having more error sources resulting from the addition of rotary axes. These errors manifest as straightness errors of the translational axis and squareness errors between the translational axes exist. Moreover, particularly in five-axis machines, positional and angular errors of the rotational center of the rotary axes also exist, according to ISO 230-1 and ISO 230-7 standards [1, 2]. Therefore, these errors must be appropriately evaluated to improve the geometrical accuracy of five-axis machines.

Many studies have investigated the motion accuracy of the rotary axes in a five-axis controlled machine tool. For example, some studies have proposed accuracy evaluation methods employing a ball-bar. The ball-bar is a device that can measure the relative motion displacement between two steel balls installed onto a spindle and a table. It is widely used as a measuring device in circular motion accuracy tests [3, 4]. Regarding the measurement method of five-axis controlled machine tools using the ball-bar, simultaneous 3- or 4-axis motions of the translational and rotary axes are proposed [5–7]. It is also clarified that the geometric errors of the rotary axes can be identified from the measured trajectories. Cone frustum cutting tests have also generally been applied to evaluate the accuracy of the five-axis machines [8]. The identical measurement test with the cone frustum cutting test employing a ball-bar has also been reported [9]. These measurement methods have been adopted as per the ISO standards published in 2014 (ISO 10791-6) [10].

The R-test device, which consists of a reference sphere and three displacement sensors, has also been proposed [11, 12]. The device has been commercially released by IBS Precision Engineering BV [13] and Fidia.S.p.A. [14]. The R-test can also evaluate the accuracy of five-axis machines [15], and the method also be adopted to meet the ISO 10791-6 standard.

While these methods can evaluate the total motion accuracy of the five-axis controlled machine tools, it is known that the measured results include the influences of both the translational and rotary axes because both these axes move simultaneously during the evaluation [16–20]. Although Ibaraki et al. [21] proposes the error map of the rotary axis, the measured results include the influence of the errors associated with translational axes.

This study seeks to appropriately evaluate both the error motions and geometric errors of the rotary axis, without involving the influence of motion error of the translational axes. Herein, only the R-test device attached to

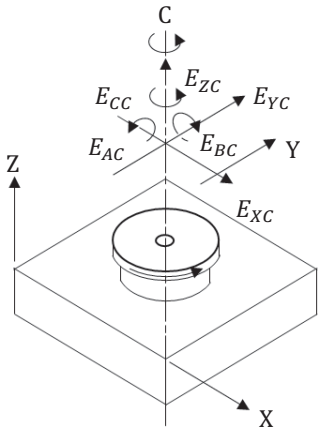

E_{XC} radial error motion of C in X-direction
E_{YC} radial error motion of C in Y-direction
E_{ZC} axial error motion of C
E_{AC} tilt error motion of C around X-axis
E_{BC} tilt error motion of C around Y-axis
E_{CC} angular positioning error motion of C

Fig. 1. Error motions of *C*-axis.

the spindle and a rotary axis is moved, while preventing synchronous motion with the translational axes. For the identification of both of the error motions and geometric errors of the *C*-axis, a rotary axis around *Z*-axis is proposed. Furthermore, the positional geometric errors of the rotary axis and the setting error of the reference sphere on the table are assumed to be factors affecting the measurement results, and the separation methods for the factors are described.

2. Error Motions and Geometric Errors of Rotary Axis

2.1. Error Motions

Error motions of a rotary axis refer to the changes in position and orientation of the axis of rotation relative to its axis average line as a function of angle of rotation of the rotary axis. These are defined in ISO 230-1 [1] and ISO 230-7 [2]. **Fig. 1** shows the error motions of the *C*-axis. Radial error motions in the *X*- and *Y*-directions and an axial error motion are positional errors of the rotational center line. Tilt error motions around the *X*- and *Y*-axes and an angular positioning error motion are angular errors of the rotational center line. As shown in **Fig. 1**, error motions are expressed by the letter *E* followed by a subscript, where the first letter refers to the name of the axis corresponding to the direction of the error motion, and the second letter refers to the axis of motion. For example, the positional error motion of the *C*-axis in the *X*-direction is represented as "E_{XC}," and the angular error motion of the *C*-axis around the *X*-axis is represented as "E_{AC}." "*A*" refers to the rotational direction around *X*-axis [1].

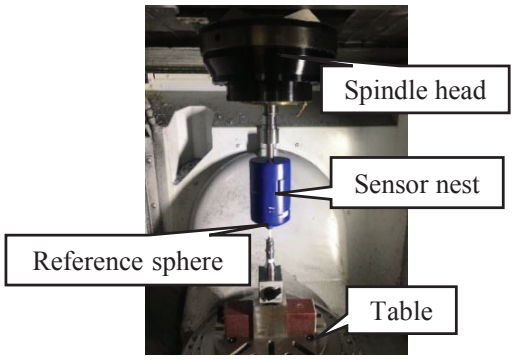

Fig. 2. Measurement set-up.

2.2. Geometric Errors

Geometric errors of a rotary axis are defined as the location and orientation errors of the axis average line of the rotary axis [1, 2]. Two positional and two orientation geometric errors can be defined for a rotary axis. Location errors of the *C*-axis in the *X*- and *Y*-directions are represented as "E_{X0C}" and "E_{Y0C}," respectively. Orientation errors around the *X*- and *Y*-axes are also represented as "E_{A0C}" and "E_{B0C}," respectively.

3. Measurement Method

In this study, error motions and geometric errors of the *C*-axis of a vertical-type five-axis machining center are identified. The five-axis machining center has *B*- and *C*-axes on the table side. **Fig. 2** shows the measurement set-up. The sensor nest is attached to the spindle, and the reference sphere is attached to the table. The center of the sensor (zero position) is set to correspond with the rotational center of the spindle. It is possible to compensate for the offset between the rotational center and the center of the sensor nest by setting the average of measured displacement of the sensors to zero while rotating the spindle. The tool length of the sensor nest is set as the length between the spindle nose and the center of the reference sphere when the sensor nest is located at the measurement height.

During the course of obtaining the measurements, the *C*-axis is rotated two times in both directions, and the measured results are averaged to identify the error motions and geometric errors. The R-test device can detect three-dimensional displacement of the reference sphere in the sensor coordinate system. The sensor coordinate system is matched with the machine coordinate system before the measurements are recorded. In case the center of the sensor nest corresponds with the designed rotational center of the *C*-axis, the measured results are influenced by the error motions and geometric errors of the *C*-axis.

To identify the angular error motions and orientation error of the axis average line, the measurement processes are conducted using two different height settings of the reference sphere, as shown in **Fig. 3**. The origin point of

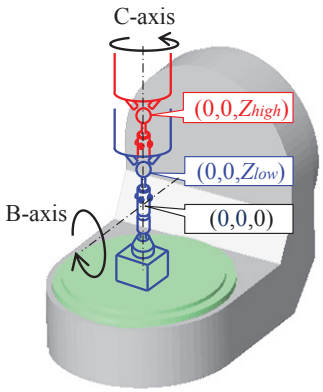

Fig. 3. Measurement setting with different height.

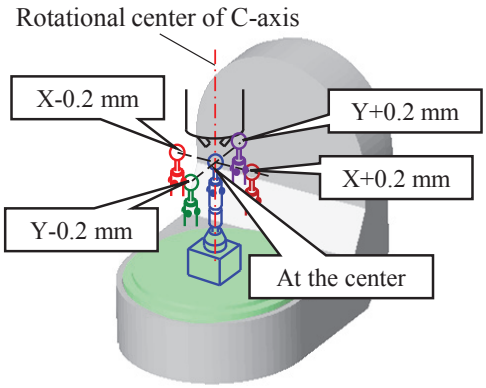

Fig. 4. Measurement test with setting error of reference sphere.

the measurement is set to be the designed cross-sectional point of the B- and C-axes. The reference sphere is set to be both the lower height Z_{low} and higher height Z_{high}.

Ideally, the center of the reference sphere should be located at the rotational center line of the C-axis. In reality, however, the center of the reference sphere is offset from the rotational center line. The offsets along the X- and Y-directions are termed "setting errors" in this study. It is expected that the setting errors affect the measured results; thus, these errors must be divided from the results.

4. Influence of Setting and Geometric Errors

4.1. Influence of Setting Error of Reference Sphere

In the real measurements, although a reference sphere is set onto the rotational center line of the C-axis, it is offset from the actual center line position. The influence of the setting error is verified to compensate for its influences. To perform the verification, simulations and experiments are conducted with an intentional offset of the reference sphere, as shown in **Fig. 4**. During the verification process, the reference sphere is set onto the table with intentional setting errors of 0.2 mm in the X-, Y-, $-X$-, and $-Y$-directions.

Figure 5 shows the simulated trajectories of the sphere in the XY-plane. As shown in the figure, the sphere moves

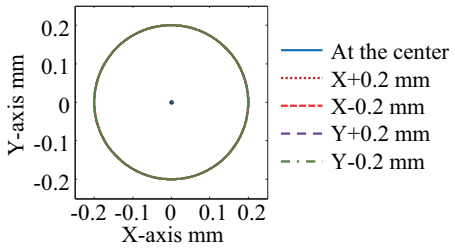

Fig. 5. Influence of sphere setting error on trajectory of sphere (simulation).

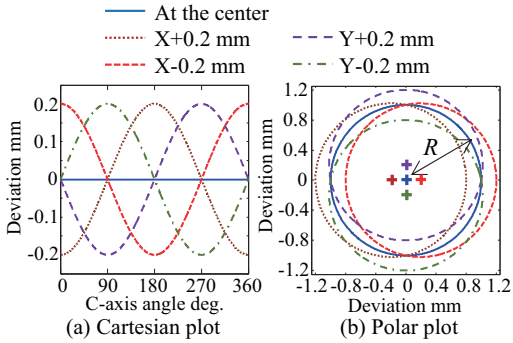

Fig. 6. Influence of sphere setting error on X-axis motion of sphere (simulation).

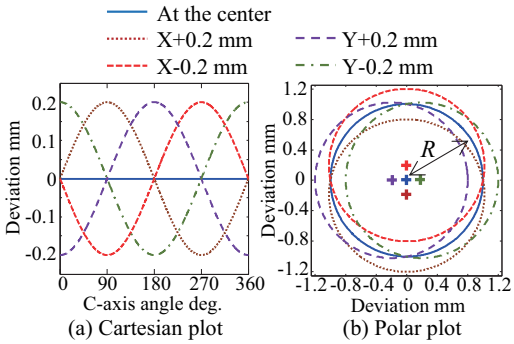

Fig. 7. Influence of sphere setting error on Y-axis motion of sphere (simulation).

on the circle with the radius of 0.2 mm. **Figs. 6** and **7** also show the displacement of the sphere along the X- and Y-directions during the motion. **Figs. 6(a)** and **7(a)** show the results with Cartesian plot representation as projections of the results shown in **Fig. 5**, and **Figs. 6(b)** and **7(b)** show the results with polar plot representation of the displacement with reference to the rotational angle of the C-axis. The radius of the circle in **Figs. 6(b)** and **7(b)** represents the vertical axis of **Figs. 6(a)** and **7(a)**. In the figures with the polar plot, the results are plotted on the reference circle with the radius of 1 mm for clarity. The figures show that the influence of the setting error can be observed as eccentricity of the circular trajectory of the X- and Y-directional displacements.

Figures 8–10 show the measured results with intentional setting errors of the sphere. Although it is impossi-

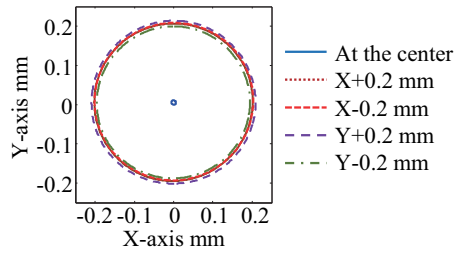

Fig. 8. Influence of sphere setting error on trajectory of sphere (experiment).

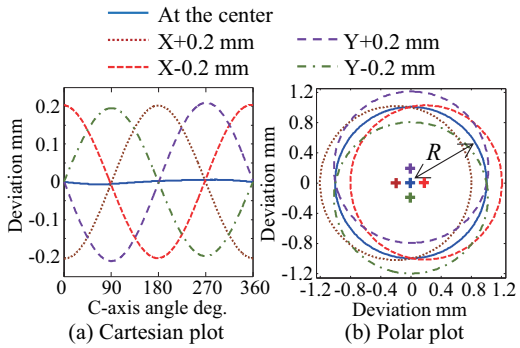

Fig. 9. Influence of sphere setting error on X-axis motion of sphere (experiment).

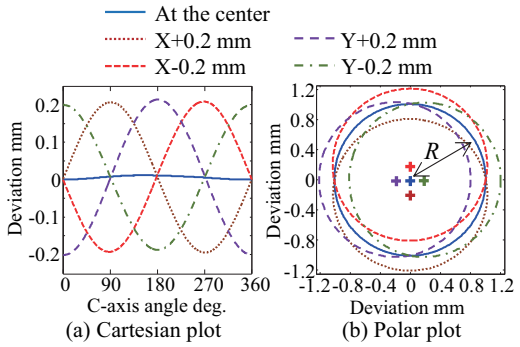

Fig. 10. Influence of sphere setting error on Y-axis motion of sphere (experiment).

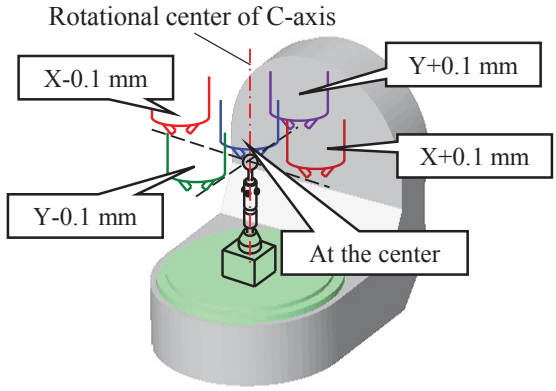

Fig. 11. Measurement with positional error of C-axis rotational center.

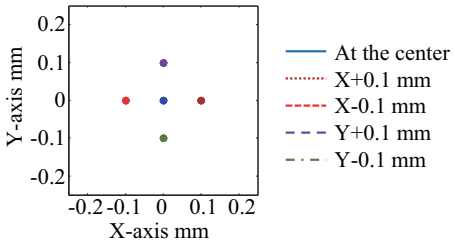

Fig. 12. Influence of C-axis positional error on trajectory of sphere (simulation).

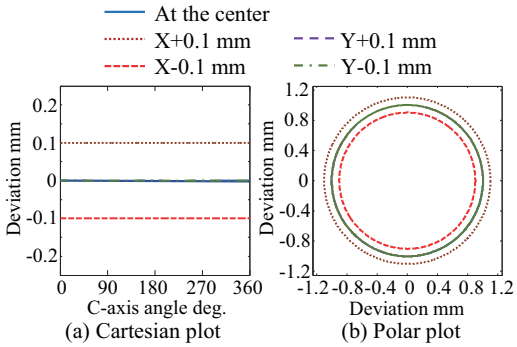

Fig. 13. Influence of C-axis positional error on X-axis motion of sphere (simulation).

ble to set the sphere with the precise offset of 0.2 mm, the sphere is set at the desired points to the maximum extent possible. According to the figures, the influence of the setting error can be observed in the same manner as that depicted by the simulated results.

4.2. Influence of Geometric Errors

Geometric errors of a rotary axis are assumed to be the differences between the designed and actual locations and orientations of the rotary axis. Therefore, the influence of the geometric errors can be expressed by change of the location of sensor nest attached to the spindle, as shown in **Fig. 11**.

Figure 12 shows the simulated trajectories of the sphere in the XY-plane with the location offset. It is assumed that the sphere is located on the rotational center line of the C-axis. As shown in the figure, the influence of geometric errors can be observed as the eccentricity of the trajectories. **Figs. 13** and **14** also show the simulated results in the X- and Y-directional displacements of the sphere during motion. **Figs. 13(a)** and **14(a)** show the results with Cartesian plot representation, and **Figs. 13(b)** and **14(b)** show the results with polar plot representation. In the figures with the polar plot, the results are plotted on the reference circle with the radius of 1 mm to depict that these are identical to the results of the influence of setting errors. The influence of geometric errors can be observed in the form of change of the radius, as shown in the figures. The X- and Y-directional offsets affect the radii of the X- and Y-directional displacements, respectively. This implies that the influence of geometric errors in the direc-

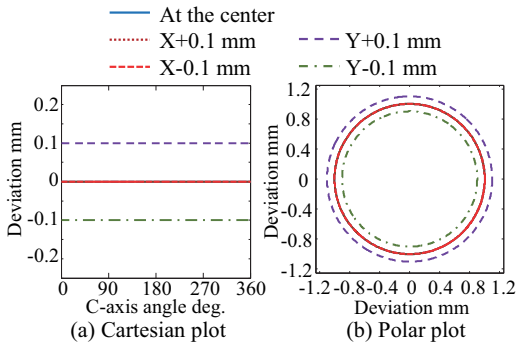

Fig. 14. Influence of C-axis positional error on Y-axis motion of sphere (simulation).

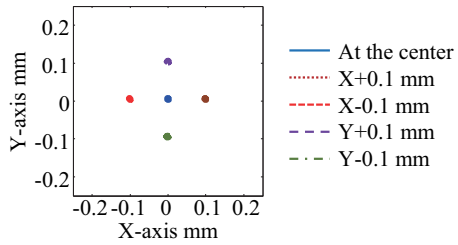

Fig. 15. Influence of C-axis positional error on trajectory of sphere (experiment).

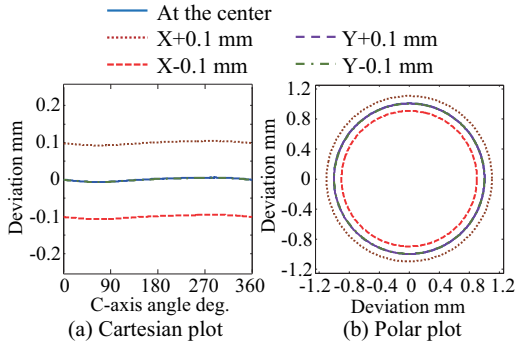

Fig. 16. Influence of C-axis positional error on X-axis motion of sphere (experiment).

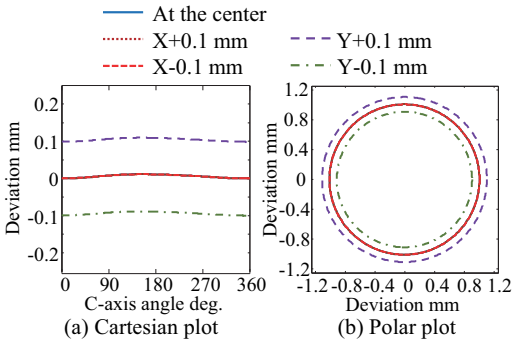

Fig. 17. Influence of C-axis positional error on Y-axis motion of sphere (experiment).

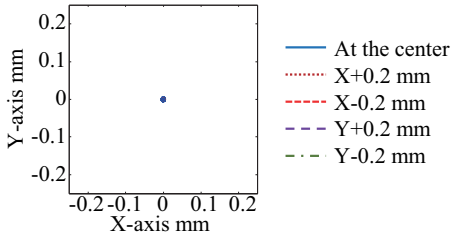

Fig. 18. Measured motion trajectories of sphere with setting error compensation.

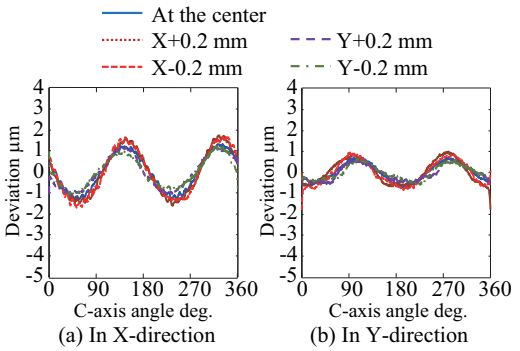

Fig. 19. Comparison of measured translational errors in case of setting error exists.

tion perpendicular to the measurement direction cannot be recognized in the figures.

Figures 15–17 show the measured results with intentional offsets of the sensor nest. According to the figures, the influence of the offset can be observed in the same manner as that depicted by the simulated results.

4.3. Separation of Error Motions and Geometric Errors

The R-test device can measure the X-, Y-, and Z-directional displacements during the motion. As mentioned earlier, the setting error of the reference sphere causes change in the eccentricity of the trajectory of the X- and Y-directional displacement, and the offset of the rotational center identical to the geometric error of the rotary axis changes the radius of the trajectory of the X- and Y-directional displacement. Therefore, it is possible to divide the influences of both the setting and geometric errors from the measured results. Resultantly, the influence of the error motions can be obtained. The obtained result is then defined as the "error motion components" in this study. The eccentricity and radius of the trajectories can be identified by applying the least square method, which is commonly used to identify such parameters.

Figures 18 and **19** show the obtained error motion components from the measured results with the setting errors shown in **Figs. 9** and **10**, respectively. **Figs. 20** and **21** also show the obtained error motion components from the measured results with geometric errors shown in **Figs. 16** and **17**, respectively. According to the figures, wave forms of the obtained error motion components are identical, even though small differences of less than 1 μm can be

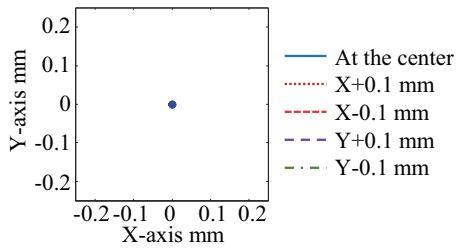

Fig. 20. Measured motion trajectories of sphere with positional error compensation.

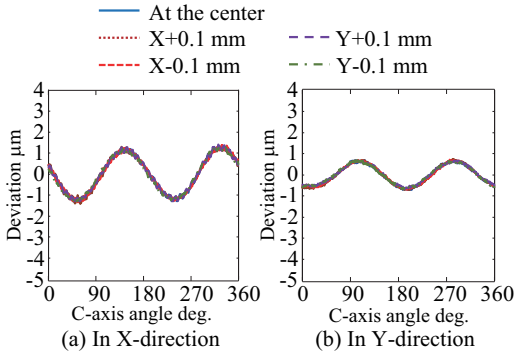

Fig. 21. Comparison of measured translational errors in case of positional error exists.

observed in the results shown in **Fig. 19**. These results confirm that the setting and geometric errors can be adequately identified by applying the least square method to the measured trajectories along the X- and Y-directions. Unfortunately, however, the reason behind the small differences observed in the results shown in **Fig. 19** have not been clarified yet.

5. Identification Method and Results

5.1. Error Motions

The error motion components can be obtained from two sets of the measured results at higher and lower measurement settings of the sphere. The measured results at two measurement heights are defined as (X_{he}, Y_{he}, Z_{he}) and (X_{le}, Y_{le}, Z_{le}), respectively.

Figure 22 shows the comparison of the measured error motion components at higher and lower measurement settings. **Fig. 22(d)** shows the radial directional errors obtained from the X- and Y-directional error motion components. It is expected that the results do not depend on the measurement height if angular error motions do not exist. According to the figure, the error motion components in the Y-direction depend on the measurement height.

Based on the error motions of the rotary axis (E_{XC}, E_{YC}, E_{ZC}, E_{AC}, and E_{BC}) and the height of the reference sphere (Z_{high} and Z_{low}), the error motion components can be represented as shown in Eq. (1). Therefore, by solving the equation on the error motions, the error motions

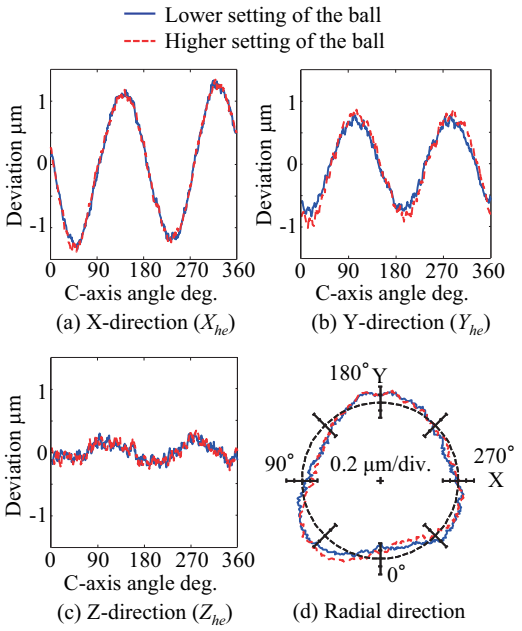

Fig. 22. Measured error motion components of C-axis.

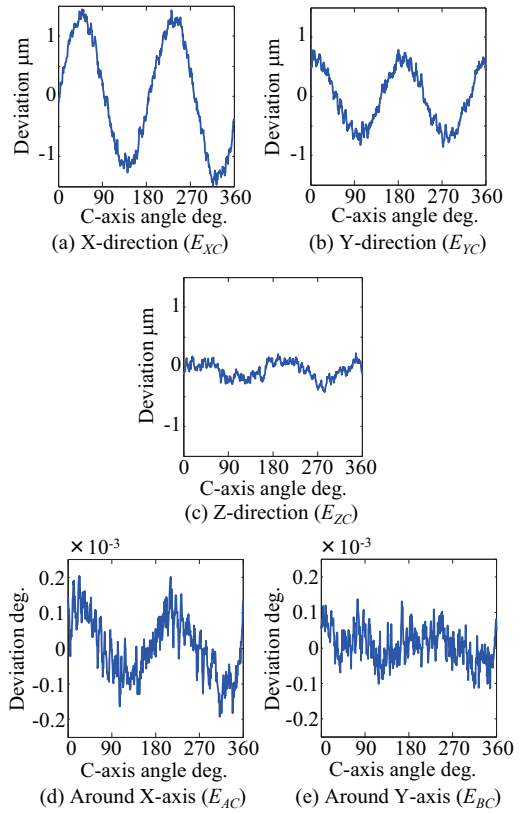

Fig. 23. Identified results of C-axis error motions.

can be obtained as shown in Eq. (2) from the measured error motion components. **Fig. 23** shows the identified results of the error motions corresponding to those when the heights of the reference sphere are $Z_{high} = 146.8$ mm and $Z_{low} = 66.7$ mm. The figures show that the five error motions except the angular positioning error motion,

Table 1. Identified geometric errors of C-axis.

	B = 0.00 deg.	B = -0.01 deg.	B = -0.02 deg.	B = -0.03 deg.
E_{A0C}	-0.00095 deg.	-0.00097 deg.	-0.00081 deg.	-0.00061 deg.
E_{B0C}	0.0011 deg.	-0.0087 deg.	-0.0187 deg.	-0.0284 deg.
E_{X0C}	2.4 µm	2.4 µm	2.4 µm	2.8 µm
E_{Y0C}	-10.0 µm	-10.0 µm	-9.6 µm	-9.4 µm

E_{CC}, can be identified from the measured result using the proposed identification method.

$$\begin{cases} (X_{he}, Y_{he}, Z_{he}) \\ \quad = (-E_{XC} + E_{BC} \cdot Z_{high}, -E_{YC} - E_{AC} \cdot Z_{high}, -E_{ZC}) \\ (X_{le}, Y_{le}, Z_{le}) \\ \quad = (-E_{XC} + E_{BC} \cdot Z_{low}, -E_{YC} - E_{AC} \cdot Z_{low}, -E_{ZC}) \end{cases} \quad \ldots\ldots\ldots\ldots\ldots\ldots\ldots\ldots (1)$$

$$\begin{cases} E_{BC} = \dfrac{X_{he} - X_{le}}{Z_{high} - Z_{low}} \\ E_{AC} = -\dfrac{Y_{he} - Y_{le}}{Z_{high} - Z_{low}} \\ E_{XC} = -X_{he} + E_{BC} \cdot Z_{high} \\ E_{YC} = -Y_{he} - E_{AC} \cdot Z_{high} \\ E_{ZC} = -Z_{he} \end{cases} \quad \ldots\ldots\ldots\ldots (2)$$

According to the figures, the radial and error motions E_{XC} and E_{YC}, respectively, fluctuate periodically, and the amplitude of the fluctuation is approximately 1 μm. The axial error motion E_{ZC} is smaller than the radial error motions. Moreover, the tilt error motions E_{BC} and E_{AC}, respectively, are approximately $1/10000°$.

5.2. Geometric Errors

The geometric errors (error of axis average line) of the rotary axis in the four directions (E_{A0C}, E_{B0C}, E_{X0C}, and E_{Y0C}) can also be identified from the measured results.

The measured positional errors of the C-axis rotational center in the X- and Y-directions at two different measurement heights are defined as CX_{high}, CY_{high}, CX_{low}, and CY_{low}, respectively. From the positional errors, the four geometric errors of the rotary axis can be calculated as shown in Eq. (3).

$$\begin{cases} E_{A0C} = \tan^{-1}\left(\dfrac{CY_{high} - CY_{low}}{Z_{high} - Z_{low}}\right) \\ E_{B0C} = \tan^{-1}\left(\dfrac{CX_{high} - CX_{low}}{Z_{high} - Z_{low}}\right) \\ E_{X0C} = CX_{low} - E_{B0C} Z_{low} \\ E_{Y0C} = CY_{low} - E_{A0C} Z_{low} \end{cases} \quad \ldots\ldots (3)$$

Here, as explained above, the positional errors can be identified by applying the least square method to the measured trajectories of the X- and Y-directions. The positional errors of the C-axis center line can be obtained as the radius of the trajectories.

To verify the effectiveness of the identification method, measurement tests were performed with intentional tilting of the C-axis. The tilt angles of the C-axis employed were $0.0°$, $-0.01°$, $-0.02°$, and $-0.03°$. The change in tilt angle implies the change in orientation error of the axis average line E_{B0C}.

Table 1 shows the comparison of the identified geometric errors for each tilt angle condition. According to the results, the orientation error around the Y-axis E_{B0C} is changed by the same extent as the tilt angle changes of the C-axis. It can thus be inferred that the proposed identification method can adequately evaluate the geometric errors without considering any motions of the translational axes. The difference between the commanded tilt angle changes and identified changes is smaller than $0.001°$. Ideally, although the other geometric errors, E_{A0C}, E_{X0C}, and E_{Y0C} should not change with the C-axis tilt angle, the errors are observed to change slightly in reality (the change is smaller than 1 μm for the location errors). Though it can be expected that the causes of these changes are the repeated recording of the measurement or the influence of the C-axis error motions, the actual cause has not been clarified yet. In future, we will attempt to clarify the factors affecting the identification accuracy of the proposed method.

6. Conclusions

This study aims to appropriately evaluate both the error motions and geometric errors of the rotary axis without considering the influence of motion errors of the translational axes. Herein, the R-test device is attached to the spindle, and only a rotary axis is moved without moving the translational axes. A method for identification of both the error motions and geometric errors of the rotary axis is proposed. In this method, the positional geometric errors of the rotary axis and the setting error of the reference sphere on the table are assumed to be factors affecting the measurement results, and these factors are divided based on the investigated results. The conclusions can be summarized as follows.

1) The influence of the setting error can be observed as eccentricity of the circular trajectory of the X- and Y-directional displacements.

2) The influence of geometric errors can be observed as change in the radius of the circular trajectory of the X- and Y-directional displacements.

3) The setting and geometric errors can adequately be identified by applying the least square method to the measured trajectories along the X- and Y-directions.

4) Five error motions except the angular positioning error motion, E_{CC}, can be identified from the measured result upon using the proposed identification method.

5) The proposed identification method can adequately evaluate the geometric errors without involving any motions of the translational axes.

It is essential to first evaluate motion accuracy to improve the overall accuracy of five-axis control machine tools. The results of this study suggest that the proposed method can comprehensively identify and evaluate both the error motions and geometric errors of the rotary axis. Furthermore, the method presents the advantage of permitting the identification without involving any effect of the translational axes.

In future, we will try to evaluate the error motions and geometric errors of the tilt axis and try to clarify the factors that affect the identification accuracy of the proposed method by comparing the results with other evaluation methods. Further, we will try to compare the results from the simultaneous three-axis motions of translational and rotary axes as specified in ISO10791-6 [11].

Acknowledgements

This study was financially supported by the Machine Tool Engineering Foundation. The authors would also like to acknowledge the extensive support of the Machine Tool Technologies Research Foundation and DMG Mori Co., Ltd.

References:

[1] ISO 230-1, "Test Code for Machine Tools – Part 1: Geometric Accuracy of Machines Operating under No-load or Quasi-static Conditions," 2012.
[2] ISO 230-7, "The Code for Machine Tools – Part 7: Geometric Accuracy of Axes of Rotation," 2015.
[3] I. Kurić, M. Košinár, and M. Císař, "Measurement and Analysis of CNC Machine Tool Accuracy in Different Location on Work Table," Proc. in Manufacturing Systems, Vol.7, pp. 259-264, 2012.
[4] ISO 230-4, "Test Code for Machine Tools – Part 4: Circular Tests for Numerically Controlled Machine Tools," 2005.
[5] M. Tsutsumi and A. Saito, "Identification and Compensation of Systematic Deviations Particular to 5-axis Machining Centres," Int. J. of Machine Tools and Manufacture, Vol.43, Issue 8, pp. 771-780, 2013.
[6] M. Tsutsumi and A. Saito, "Identification of Angular and Positional Deviations to 5-axis Machining Centres with a Tilting-rotary Table by Four-axis Controlled Movements," Int. J. of Machine Tools and Manufacture, Vol.44, Issue 12, pp. 1333-1342, 2014.
[7] M. Tsutsumi, S. Tone, N. Kato, and R. Sato, "Enhancement of Geometric Accuracy of Five-axis Machining Centers Based on Identification and Compensation of Geometric Deviations," Int. J. of Machine Tools and Manufacture, Vol.68, pp. 11-20, 2013.
[8] NAS 979, "Uniform Cutting Tests – Metal Cutting Equipment Specifications," Aerospace Industries Association of America, pp. 34-37, 1969.
[9] N. Kato, M. Tsutsumi, and R. Sato, "Analysis of Circular Trajectory Equivalent to Cone-frustum Milling in Five-axis Machining Centers," Int. J. of Machine Tools and Manufacture, Vol.64, pp. 1-11, 2013.
[10] Y. Ihara, K. Tsuji, and T. Tajima, "Ball bar Measurement of Motion Accuracy in Simulation Cone Frustum Cutting on Multi-axis Machine Tools," Int. J. Automation Technol., Vol.11, No.2, pp. 197-205, 2017.
[11] ISO 10791-6, "Machine tools – Test conditions for machining centres – Part 6: Accuracy of speeds and interpolations," 2014.
[12] S. Weikert, "R-test, a New Device for Accuracy Measurements on Five Axis Machine Tools," CIRP Ann.-Manuf. Technol., Vol.53, Issue 1, pp. 429-432, 2004.
[13] IBS Precision Engineering BV. http://www.ibspe.com [Accessed September 14, 2019].
[14] Fidia.S.p.A. http://www.fidia.it [Accessed September 14, 2019].
[15] B. Bringmann and W. Knapp, "Model-based 'Chase-the ball' Calibration of a 5-axes Machining Center," Annals of the CIRP, Vol.55, Issue 1, pp. 531-534, 2006.
[16] C. Hong, S. Ibaraki, and A. Matsubara, "Influence of Position-dependent Geometric Errors of Rotary Axes on a Machining Test Cone Frustum by Five-axis Machine Tools," Precision Engineering, Vol.35, Issue 1, pp. 1-11, 2011.
[17] L. Zhong, Q. Bi, and Y. Wang, "Volumetric Accuracy Evaluation for Five-axis Machine Tools by Modeling Spherical Deviation Based on Double Ball-bar Kinematic Test," Int. J. of Machine Tools and Manufacture, Vol.122, pp. 106-119, 2017.
[18] B. Bringmann and W. Knapp, "Machine Tool Calibration: Geometric Test Uncertainty Depends on Machine Tool Performance," Precision Engineering, Vol.33, Issue 4, pp. 524-529, 2009.
[19] M. Yamaji, N. Hamabata, and Y. Ihara, "Evaluation of Linear Axis Motion Error of Machine Tools Using an R-test Device," Procedia CIRP, Vol.14, pp. 311-316, 2014.
[20] G. H. J. Florussen, H. A. M. Spaan, and T. M. Spaan-Burke, "Verifying the Accuracy of Five-axis Machine Tool Focused on Kinematic ISO Tests Using a Torus-Shaped Test Work Piece," Procedia Manufacturing, Vol.14, pp. 58-65, 2017.
[21] S. Ibaraki, C. Oyama, and H. Otsubo, "Construction of an Error Map of Rotary Axes on a Five-axis Machining Center by Static R-test," Int. J. of Machine Tools and Manufacture, Vol.51, Issue 3, pp. 190-200, 2011.

Name:
Takaaki Kenno

Affiliation:
Graduate Student, Graduate School of Engineering, Kobe University

Address:
1-1 Rokko-dai, Nada, Kobe 657-8501, Japan

Brief Biographical History:
2018- Master Course Student, Kobe University
2019- Kubota Co., Ltd.

Main Works:
• "Influence of Linear Axis Error Motions on Simultaneous Three-axis Controlled Motion Accuracy Defined in ISO 10791-6," Precision Engineering, Vol.61, pp. 110-119, 2020.

Membership in Academic Societies:
• Japan Society for Precision Engineering (JSPE)

Name:
Ryuta Sato

Affiliation:
Associate Professor, Department of Mechanical Engineering, Graduate School of Engineering, Kobe University

Address:
1-1 Rokko-dai, Nada, Kobe 657-8501, Japan

Brief Biographical History:
2004- Research Associate, Tokyo University of Agriculture and Technology
2008- Researcher, Mitsubishi Electric Corporation
2010- Assistant Professor, Kobe University
2013- Associate Professor, Kobe University

Main Works:
• "Finished Surface Simulation Method to Predicting the Effects of Machine Tool Motion Errors," Int. J. Automation Technol., Vol.8, No.6, pp. 801-810, 2014.
• "Influence of Motion Errors of Feed Drive Systems on Machined Surface," J. of Advanced Mechanical Design, Systems, and Manufacturing, Vol.6, No.6, pp. 781-791, 2012.
• "Generation Mechanism of Quadrant Glitches and Compensation for it in Feed Drive Systems of NC Machine Tools," Int. J. Automation Technol., Vol.6, No.2, pp. 154-162, 2012.

Membership in Academic Societies:
• Japan Society of Mechanical Engineers (JSME)
• Japan Society for Precision Engineering (JSPE)
• Society of Instrument and Control Engineers (SICE)

Name:
Keiichi Shirase

Affiliation:
Professor, Department of Mechanical Engineering, Graduate School of Engineering, Kobe University

Address:
1-1 Rokko-dai, Nada, Kobe 657-8501, Japan

Brief Biographical History:
1984- Research Associate, Kanazawa University
1995- Associate Professor, Kanazawa University
1996- Associate Professor, Osaka University
2003- Professor, Kobe University

Main Works:
• K. Shirase and K. Nakamoto, "Simulation Technologies for the Development of an Autonomous and Intelligent Machine Tool," Int. J. Automation Technol., Vol.7, No.1, pp. 6-15, 2013.
• T. Kobayashi, T. Hirooka, A. Hakotani, R. Sato, and K. Shirase, "Tool Motion Control Referring to Voxel Information of Removal Volume Voxel Model to Achieve Autonomous Milling Operation," Int. J. Automation Technol., Vol.8, No.6, pp. 792-800, 2014.
• M. M. Isnaini, Y. Shinoki, R. Sato, and K. Shirase, "Development of CAD-CAM Interaction System to Generate a Flexible Machining Process Plan," Int. J. Automation Technol., Vol.9, No.2, pp. 104-114, 2015.
• K. Shirase, "CAM-CNC integration for innovative intelligent machine tool," Proc. of the 8th Int. Conf. on Leading Edge Manufacturing in 21st Century (LEM21), A01, 2015.
• I. Nishida, R. Okumura, R. Sato, and K. Shirase, "Cutting Force Simulation in Minute Time Resolution for Ball End Milling Under Various Tool Posture," ASME J. of Manufacturing Science and Engineering, Vol.140, No.2, 021009, 2018.

Membership in Academic Societies:
• American Society of Mechanical Engineers (ASME)
• Society of Manufacturing Engineers (SME)
• Japan Society of Mechanical Engineers (JSME), Fellow
• Japan Society for Precision Engineering (JSPE), Fellow

Name:
Shigemasa Natsume

Affiliation:
P&C Ltd.

Address:
10F, Nisso 5 Bldg., 2-10-39 Kitasaiwai, Nishi-ku, Yokohama, Kanagawa 220-0004, Japan

Brief Biographical History:
1996- Department of Mechanical System Engineering, Kanagawa Institute of Technology
2000- Measurement Systems Division, Japan Ade Ltd.
2012- Japan Technical Center, Lion Precision
2015- P&C Ltd.

Main Works:
• "Influence of Linear Axis Error Motions on Simultaneous Three-axis Controlled Motion Accuracy Defined in ISO 10791-6," Precision Engineering, Vol.61, pp. 110-119, 2020.

Membership in Academic Societies:
• Field support of capacitive and eddy current sensor with experience for around 20 years as engineering
• Sales and Engineering (IBS Precision Engineering, Lion Precision, Professional Instruments)

Name:
Henny Spaan

Affiliation:
IBS Precision Engineering BV

Address:
201 Esp, Eindhoven 5633AD, Netherlands

Brief Biographical History:
1990 Received Master of Science degree (Mechanical Engineering) from Eindhoven University of Technology
1993- Founder/President, IBS Precision Engineering BV
1995 Received Doctoral degree (Mechanical Engineering) from Eindhoven University of Technology

Main Works:
• Several patents on machine tool error calibration and compensation techniques
• (Ultra-precision) metrology
• Received Rien Koster Award (Dutch) in 2013 for his contribution to mechatronics and precision technology
• ISO (TC213: Metrology)

Membership in Academic Societies:
• International Academy for Production Engineering (CIRP)
• European Society for Precision Engineering and Nanotechnology (euspen)
• American Society for Precision Engineering (ASPE), former Board Member
• Mechanical Engineering Industry Association (VDMA) Electronics, Micro and New Energy Production Technologies (EMINT), Board Member